MPMI Vol. 37, No. 2, 2024, pp. 143–154, https://doi.org/10.1094/MPMI-10-23-0153-R

Ectopic Expression of the Executor-Type *R* Gene Paralog *Xa27B* in Rice Leads to Spontaneous Lesions and Enhanced Disease Resistance

Dongsheng Tian,[1] Joanne Teo,[1] and Zhongchao Yin[1,2,†]

[1] Temasek Life Sciences Laboratory, National University of Singapore, Singapore 117604, Republic of Singapore
[2] Department of Biological Sciences, National University of Singapore, Singapore 117543, Republic of Singapore

Accepted for publication 2 December 2023.

Plant disease resistance (*R*) gene-mediated effector-triggered immunity (ETI) is usually associated with hypersensitive response (HR) and provides robust and race-specific disease resistance against pathogenic infection. The activation of ETI and HR in plants is strictly regulated, and improper activation will lead to cell death. *Xa27* is an executor-type *R* gene in rice induced by the TAL effector AvrXa27 and confers disease resistance to *Xanthomonas oryzae* pv. *oryzae* (*Xoo*). Here we reported the characterization of a transgenic line with lesion mimic phenotype, designated as *Spotted leaf and resistance 1* (*Slr1*), which was derived from rice transformation with a genomic subclone located 5,125 bp downstream of the *Xa27* gene. *Slr1* develops spontaneous lesions on its leaves caused by cell death and confers disease resistance to both *Xoo* and *Xanthomonas oryzae* pv. *oryzicola*. Further investigation revealed that the *Slr1* phenotype resulted from the ectopic expression of an *Xa27* paralog gene, designated as *Xa27B*, in the inserted DNA fragment at the *Slr1* locus driven by a truncated CaMV35Sx2 promoter in reverse orientation. Disease evaluation of IRBB27, IR24, and *Xa27B* mutants with *Xoo* strains expressing dTALE-Xa27B confirmed that *Xa27B* is a functional executor-type *R* gene. The functional XA27B-GFP protein was localized to the endoplasmic reticulum and apoplast. The identification of *Xa27B* as a new functional executor-type *R* gene provides additional genetic resources for studying the mechanism of executor-type R protein-mediated ETI and developing enhanced and broad-spectrum disease resistance to *Xoo* through promoter engineering.

Keywords: bacterial blight, executor-type *R* gene, rice, *Xa27*, *Xa27B*, *Xanthomonas oryzae* pv. *oryzae*

Plants evolve two layers of interdependent immunity in response to pathogen infection: pattern-triggered immunity (PTI) and effector-triggered immunity (ETI) (Ngou et al. 2021, 2022; Yuan et al. 2021). During PTI, the host cell surface-localized pattern-recognition receptors sense pathogen-associated molecular patterns, which are evolutionarily conserved microbial molecular signatures derived from the pathogens, and activate downstream immune responses, including Ca^{2+} influx, reactive oxygen species (ROS) burst, mitogen-activated protein kinase activation, production of phytohormones, guard cell closure, cell wall thickening, transcriptional reprogramming, and phytohormone signaling (Bigeard et al. 2015). To circumvent or overcome PTI, pathogens deliver effector proteins into host cells, where they interfere with or suppress defense responses, eventually leading to effector triggered susceptibility (ETS). To counteract ETS, plants evolve resistance (*R*) genes whose products act as cytoplasmic immune receptors that recognize pathogen effectors directly or indirectly, leading to the activation of ETI (Ngou et al. 2022). ETI often accompanies hypersensitive response (HR), a localized rapid host cell death occurring at the site of pathogen infection (Balint-Kurti 2019). Compared with PTI, which provides a mild overall disease resistance in plants, the immune responses of ETI are more specific, robust, and prolonged. In addition, in the absence of pathogens, the activation of ETI and HR must be suppressed completely, because their improper activation will lead to cell death and growth retardation (Balint-Kurti 2019; Tang et al. 1999; Tian and Yin 2009).

Bacterial blight, caused by *Xanthomonas oryzae* pv. *oryzae* (*Xoo*), is one of the most destructive bacterial diseases in rice and causes significant yield loss (Niño-Liu et al. 2006). *Xoo* strains rely on diverse members of the AvrBs3 family-type III effectors, also called transcription activator-like (TAL) effectors, for virulence (Yang and White 2004). TAL effectors have a modular structure with an N-terminal secretion signal, a central DNA-binding domain comprising a tandem array of nearly identical repeats with each at 33 at 34 residues, and a C-terminal region containing nuclear localization signals and a transcriptional activation domain (Bogdanove et al. 2010). The polymorphism at residue numbers 12 and 13, also termed repeat variable di-residues (RVDs), in each repeat and the array of repeats determine the DNA-binding specificity (Boch et al. 2009; Moscou and Bogdanove 2009). TAL effectors bind to the promoters of susceptibility (*S*) genes and induce *S* gene expression to promote disease development (Antony et al. 2010; Chu et al. 2006; Sugio et al. 2007; Yang et al. 2006). Rice and its wild relatives have evolved TAL effector-dependent dominant *R* genes, also known as executor-type *R* genes, to counteract TAL effector-dependent disease susceptibility (Zhang et al. 2015). Unlike conventional *R* genes, the resistance specificity of an executor-type *R* gene is determined by the effector binding element (EBE) in its promoter and the tandem arranged repeats located in the center of

[†]Corresponding author: Z. Yin; yinzc@tll.org.sg

Author contributions: D.T. and Z.Y. designed the research. D.T. and J.T. conducted the experiments. D.T. and Z.Y. analyzed the data and wrote the manuscript.

Funding: Funding was provided by intramural research funds from the Temasek Life Sciences Laboratory.

***e*-Xtra:** Supplementary material is available online.

The author(s) declare no conflict of interest.

the cognate TAL effector. The executor-type *R* genes encode highly toxic proteins that trigger HR and activate disease resistance (Chen et al. 2021; Gu et al. 2005; Luo et al. 2021; Tian et al. 2014; Wang et al. 2015, 2021). Because of their high toxicity, the expression of executor-type *R* genes is strictly suppressed in the absence of incompatible *Xoo* strains, as ectopic or constitutive expression of executor-type *R* genes in rice would cause cell death with spontaneous lesions, growth retardation, and even death of plants (Gu et al. 2005; Tian and Yin 2009).

The bacterial blight *R* gene *Xa27* and its cognate avirulence (*Avr*) TAL effector gene *avrXa27* were isolated from rice line IRBB27 and *Xoo* strain PXO99^{A}, respectively (Gu et al. 2005). XA27 is a small and novel protein with three transmembrane helix domains and an N-terminal signal anchor-like sequence, which is required for its localization to the apoplast of rice cells for conferring disease resistance to *Xoo* strains (Wu et al. 2008). Histological study also indicated that secondary cell wall thickening occurred in vascular bundle elements in IRBB27 plants during incompatible interaction as well as in *Xa27* ectopic expression lines (Gu et al. 2005; Tian and Yin 2009). XA27 has four putative paralog proteins in 'Nipponbare', a susceptible cultivar of the *japonica* subspecies to *Xa27*-incompatible *Xoo* strain PXO99^{A} (Gu et al. 2005). Previously, designer TAL effectors (dTALEs) were made to induce the expression of the four *Xa27* paralog genes in Nipponbare. However, none of them could confer disease resistance to the *Xoo* strains expressing the corresponding dTALEs, indicating that the four XA27 paralog proteins have lost their function in activating disease resistance signaling (Li et al. 2013). In this study, we report the identification of *Xa27B*, a functional *Xa27* paralog gene in IRBB27 and IR24. The constitutive expression of *Xa27B* in rice caused a lesion mimic phenotype and conferred enhanced and broad-spectrum disease resistance to *Xoo* and *Xanthomonas oryzae* pv. *oryzicola* (*Xoc*).

Results

The transgenic line *Slr1* develops spontaneous lesions and confers enhanced disease resistance to *Xoo* and *Xoc*

In the previous study, we reported the isolation of bacterial blight *R* gene *Xa27* by map-based cloning approach through genetic complementation with genomic subclones at the *Xa27* locus (Gu et al. 2005). One of the genomic subclones tested for genetic complementation study was PP12, a 11909-bp *Pst*I fragment located 5,125 bp downstream of the *Xa27* gene. Transgenic T0 plants harboring PP12 were subjected to bacterial blight inoculation. Out of the 60 T0 plants evaluated, 59 were susceptible to *Xoo* strain PXO99^{A}. The remaining T0 plant, T0-43, exhibited a lesion mimic phenotype on its leaves and conferred disease resistance to *Xoo* strain PXO99^{A} (Fig. 1A and B). T0-43 was designated as *Spotted leaf and resistance 1* (*Slr1*). Genetic analysis indicated that the lesion mimic phenotype was co-segregated with the hygromycin resistance or T-DNA in the T1 generation (data not shown). In an *Slr1* T2 segregating population ($n = 255$), the lesion mimic phenotype and disease resistance to *Xoo* strain PXO99^{A} were co-segregated and inherited in a dominant manner with a 3:1 Mendelian ratio ($\chi^2 = 0.03$, $P = 0.86$) (Table 1). The results demonstrated that either a transgene on T-DNA or T-DNA insertional mutation at the *Slr1* locus caused the lesion mimic phenotype and disease resistance to *Xoo* strain PXO99^{A}.

The spontaneous lesions on *Slr1* plants developed progressively, starting with yellowish lesions on the leaf blade of the second leaf at 2 weeks after sowing, increasing in size and number, spreading from the leaf tip to the leaf base, and eventu-

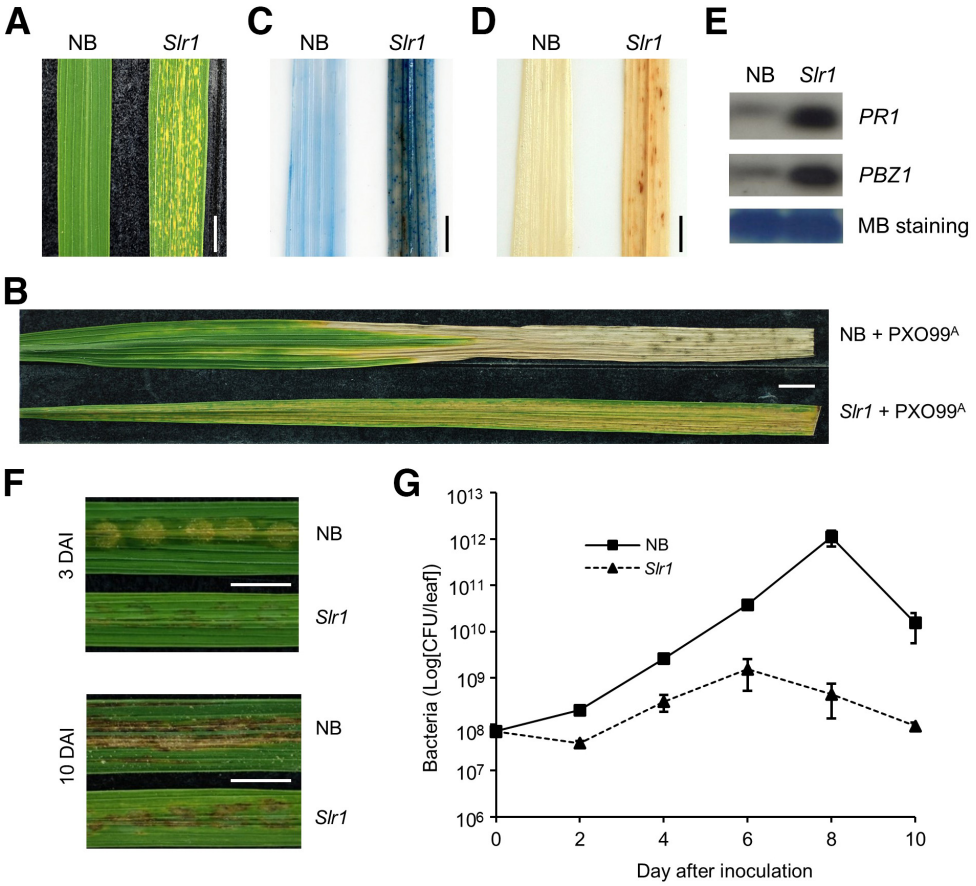

Fig. 1. Characterization of *Slr1*. **A,** Phenotype of leaves of Nipponbare and *Slr1*. NB, Nipponbare; *Slr1*, hemizygous progeny derived from T0-43. **B,** Phenotype of bacterial blight on leaves of Nipponbare and *Slr1* at 14 days after inoculation (DAI) with *Xanthomonas oryzae* pv. *oryzae* (*Xoo*) strain PXO99^{A}. **C,** Trypan blue staining of leaves of Nipponbare and *Slr1*. **D,** 3,3′-Diaminobenzidine (DAB) staining of leaves of Nipponbare and *Slr1*. **E,** Expression of *PR1* and *PBZ1* genes in leaves of Nipponbare and *Slr1* detected by Northern blot analysis. RNA loading control was stained with methanol blue (MB). **F,** Phenotype of bacterial leaf streak on leaves of Nipponbare and *Slr1* at 3 DAI (top) and 10 DAI (bottom) with *Xoc* strain L8. **G,** Bacterial population of *Xanthomonas oryzae* pv. *oryzicola* (*Xoc*) strain L8 in leaves of Nipponbare and *Slr1* over 10 DAI. Scale bars: 1 cm.

ally covering the entire leaf blade. The homozygous *Slr1* plants had a severe lesion mimic phenotype with substantial growth retardation and usually died before entering the reproductive stage. Therefore, the *Slr1* plants were mainly maintained as hemizygotes. Lesion mimic mutants are usually associated with cell death and activation of defense responses, including accumulation of ROS and constitutive expression of defense genes (Lorrain et al. 2003; Zhang et al. 2022). Cell death was detected on *Slr1* leaves, especially in the lesion areas, by trypan blue staining, whereas only background staining was observed on the leaves of Nipponbare (Fig. 1C). The accumulation of H_2O_2, a non-radical ROS, was detected as reddish-brown precipitates on the *Slr1* leaves by 3,3′-diaminobenzidine (DAB) staining (Fig. 1D). No H_2O_2 accumulation was detected on the healthy leaves of Nipponbare (Fig. 1D). The expression of the *PR1* and *PBZ1* genes, two typical pathogenesis-related genes for defense response to pathogen infection, were highly activated in *Slr1* plants, while only background expression of the two defense genes was detected in Nipponbare (Fig. 1E). The constitutive activation of defense response in *Slr1* plants also provided enhanced disease resistance to *Xoc* strain, the causal agent of bacterial leaf streak (BLS) in rice (Fig. 1F and G). Compared with effects observed in Nipponbare, which was completely susceptible to *Xoc* strain L8, the development of BLS on *Slr1* leaves was much slower and no yellow beads of *Xoc* were observed on *Slr1* leaves at 10 days after inoculation (DAI) (Fig. 1F). In addition, the bacterial population of *Xoc* strain L8 was significantly higher in Nipponbare plants than in *Slr1* plants, with the difference ranging from 5.2-fold at 2 DAI to 2,503.5-fold at 8 DAI (Fig. 1G). The results demonstrate that the lesion mimic phenotype on *Slr1* plants resulted from cell death caused by ROS accumulation and the constitutive activation of defense response conferred enhanced and broad-spectrum disease resistance to both *Xoo* and *Xoc*.

The lesion mimic phenotype on *Slr1* plants results from the ectopic expression of the *Xa27B* gene

The lesion mimic phenotype and disease resistance of the *Slr1* plants were co-inherited as a single-locus dominant trait (Table 1). Two hybridization bands for the T0-43 plant were detected in Southern blot analysis by a DNA probe derived from the hygromycin phosphotransferase (*Hpt*) gene, and they co-segregated in the T2 segregating population (Supplementary Fig. S1). The results indicate that there are at least two copies of T-DNAs in the T0-43 plant, and they might be inserted in the rice genome at the exact or a closely related location. A bacterial artificial chromosome (BAC) clone (M180P09) harboring the inserted T-DNA fragment at the *Slr1* locus was isolated from a homemade BAC library of *Slr1* (data not shown). The DNA insert in M180P09 was sequenced and compared with the genome sequence of Nipponbare at the insertion site. A 6,026-bp DNA fragment was found to be inserted into an intergenic region between LOC_Os11g42120 and LOC_Os11g42130 on chromosome 11 of Nipponbare (Fig. 2A). The 6,026-bp inserted DNA fragment contained four copies of truncated T-DNAs derived from the T-DNA region in the binary construct pC1300PP12 harboring the subclone PP12, possibly through illegitimate T-DNA integration (Fig. 2A and B). Among the four copies of the truncated T-DNAs, two copies containing only the *Hpt* genes, with one on each side of the 6,026-bp inserted DNA fragment, were inserted in opposite orientations to each other (Fig. 2A and B). The two *Hpt* genes carried truncated CaMV35Sx2 promoters (2x35S promoter or P_{2x35S}) of 398 bp ($P_{t2x35S1}$) and 583 bp ($P_{t2x35S2}$), respectively, which were derived from the *Hpt* gene in the T-DNA region of pC1300PP12 (Fig. 2B). The other two truncated T-DNAs had molecular sizes of 595 bp and 1,689 bp, respectively, and were inserted in the middle of the 6,026-bp inserted DNA fragment and flanked by the two *Hpt* genes (Fig. 2A and B). Both the 595-bp and the 1,689-bp DNA fragments were derived from the subclone PP12 but were inserted at the *Slr1* locus in reverse orientation (Fig. 2B). The 595-bp DNA fragment was derived from the first intron of the rice gene LOC_Os06g39760 and designated as 595IPI (595-bp inverted partial intron fragment) (Fig. 2B). Manual gene annotation with the 1,689-bp DNA fragment identified a 348-bp open reading frame (ORF) that encodes an XA27 paralog protein. The *Xa27* paralog gene was designated as *Xa27B* (Fig. 2A and B). Subclones derived from M180P09 that harbored either the 6,026-bp inserted fragment (H20015) or the *Xa27B* gene (X8291 and XX2654) produced transgenic plants with lesion mimic phenotype (Figs. 2A and 3A). Like *Slr1* plants, the transgenic plants harboring the shortest subclone XX2654 also conferred disease resistance to the *Xoo* strain PXO99^A (Fig. 3B). The results indicate that the *Xa27B* gene is the functional candidate gene at the *Slr1* locus that causes lesion mimic phenotype and confers enhanced disease resistance to *Xoo* and *Xoc*.

The full-length cDNA of the *Xa27B* gene, which was 618 bp, including a 43-bp 5′ untranslated region (UTR), the 348-bp ORF, and a 227-bp 3′ UTR, was isolated from the *Slr1* plants (Supplementary Fig. S3). qRT-PCR analysis revealed that the *Xa27B* gene was constitutively expressed in the *Slr1* plants as well as in the transgenic plants harboring subclone XX2654 (Fig. 3C). The *Xa27B* transcript was almost undetectable in IRBB27 plants (Cq = 36.1 ± 0.7) (Fig. 3C). No *Xa27B* transcript was detected in Nipponbare, as it does not carry the *Xa27B* allele (Fig. 3C). To examine whether the constitutive expression of the *Xa27B* gene in *Slr1* plants could provide enhanced and broad-spectrum disease resistance to *Xoo* strains, we inoculated Nipponbare and *Slr1* plants with four *Xa27*-incompatible *Xoo* strains (PXO99^A, A3842, HB21, and T7174) and three *Xa27*-compatible *Xoo* strains (1947, K202, and ZHE173) (Gu et al. 2004). Disease evaluation indicated that the *Slr1* plants conferred disease resistance to the seven *Xoo* strains tested (Fig. 3D).

The truncated 2x35S promoter ($P_{t2x35S1}$) drives *Xa27B* expression in *Slr1* plants in reverse orientation

The *Xa27B* gene in the 6,026-bp inserted DNA fragment and its subclone XX2654 contains a 412-bp 5′ regulation region (P_{Xa27B}), including the 43-bp 5′ UTR, and a 929-bp 3′ regulation region, including the 227-bp 3′ UTR (Supplementary Fig. S3). As the subclone XX2654 produced transgenic plants with constitutive expression of the *Xa27B* gene and lesion mimic phenotype,

Table 1. Lesion mimic phenotype of *Slr1* T2 plants and disease evaluation for bacterial blight resistance

Lesion mimic phenotype and disease evaluation[a]	Number of T2 plants
LM$^+$ and R	190
LM$^-$ and S	65
LM$^+$ and S	0
LM$^-$ and R	0
χ^2 (3:1)	0.03
P	0.86

[a] Plants derived from *Slr1* T2 segregating population were inoculated with *Xanthomonas oryzae* pv. *oryzae* (*Xoo*) strain PXO99^A and bacterial blight phenotypes were scored at 14 days after inoculation (DAI) according to the criteria described in "Materials and Methods." The phenotypes of T2 plants were categorized as follows: LM$^+$ and R, positive lesion mimic phenotype and resistant to *Xoo* strain PXO99^A; LM$^-$ and S, negative lesion mimic phenotype and susceptible to *Xoo* strain PXO99^A; LM$^+$ and S, positive lesion mimic phenotype and susceptible to *Xoo* strain PXO99^A; LM$^-$ and R, negative lesion mimic phenotype and resistant to *Xoo* strain PXO99^A. The segregation ratio considered and the chi-square goodness-of-fit test are indicated.

we examined the promoter activity of the $P_{t2x35S1}$-595IPI-P_{Xa27B} fragment and its deletion variants upstream of the *Xa27B* coding region in XX2654 using a promoter-less GUS reporter system in binary construct pC1305.1D2 (Fig. 4). pC1305.1D2 was derived from the binary vector pC1305.1 and did not produce any GUS activity in infiltrated *Nicotiana benthamiana* leaves (Fig. 4). The full-length P_{2x35S}-595IPI-P_{Xa27B} fragment had promoter activity that produced GUS activity in infiltrated *N. benthamiana* leaves, whereas the 595IPI-P_{Xa27B} fragment or the P_{Xa27B} promoter alone abolished promoter activity (Fig. 4). The results in-

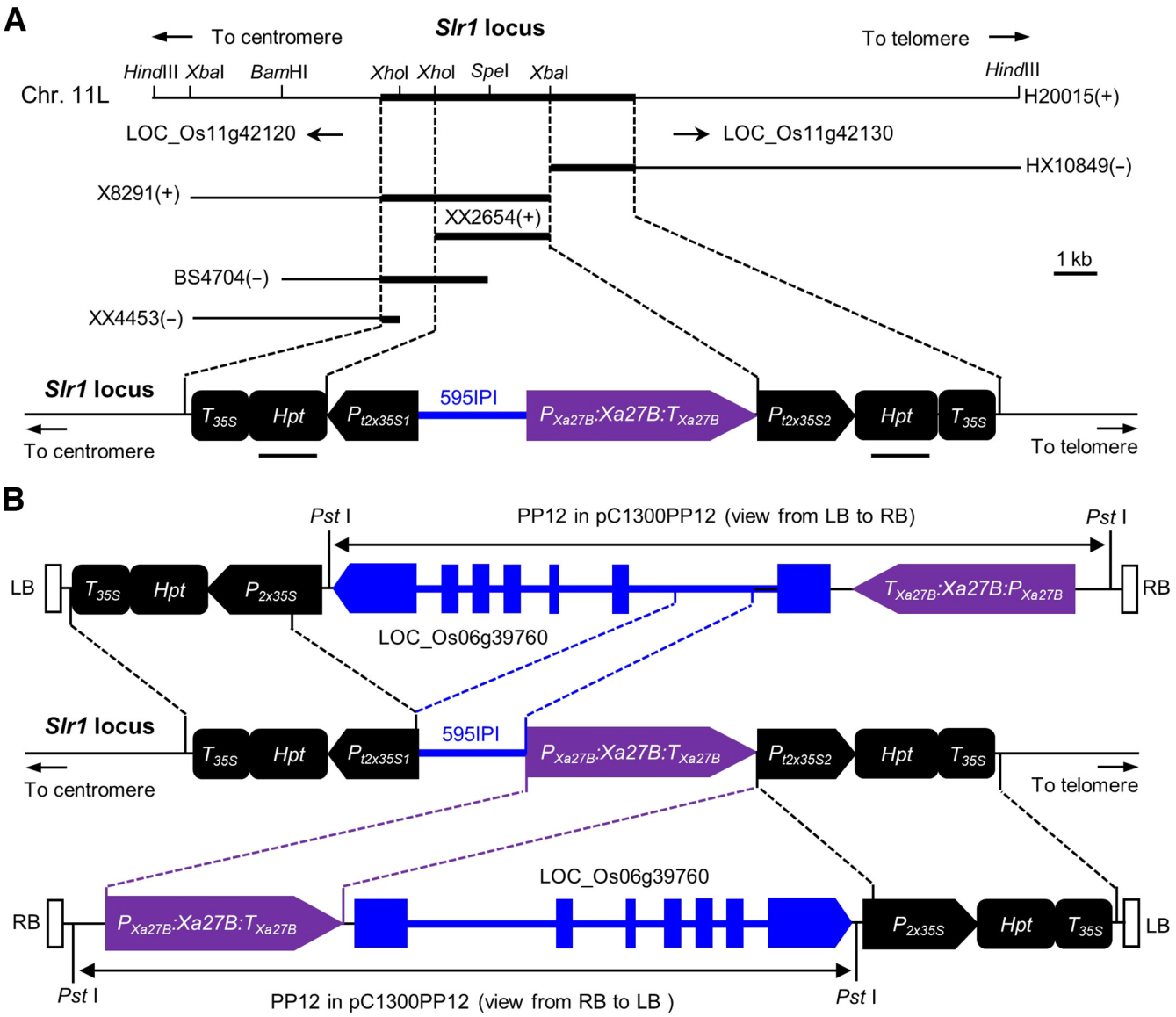

Fig. 2. Identification of *Xa27B* at the *Slr1* locus. **A,** Physical and schematic maps of the multiple truncated T-DNAs at the *Slr1* locus and their flanking rice genomic sequences. H20015, HX10849, X8291, XX2654, BS4704, and XX4453 are subclones of the BAC clone M180P09. The 6,026-bp inserted DNA fragment is shown as a black bold line. Two hypothetical genes LOC_Os11g42120 and LOC_Os11g421130 flanking the 6,026-bp inserted DNA fragment are marked below the subclone H20015 with arrowheads indicating the orientation of transcription. H20015 is marked with restriction enzyme digestion sites. Dotted lines denote the locations of subclones. Subclones that produced lesion mimic transgenic plants are indicated with a plus (+). Otherwise, they are marked with a minus (–). The colored schematic map shows the DNA elements in the 6,026-bp inserted DNA fragment at the *Slr1* locus (see also in B). The DNA probes derived from the *Hpt* gene for Southern blot analysis are indicated under the *Hpt* coding regions below the schematic map. **B,** Schematic map showing the origins of the DNA elements in the 6,026-bp inserted DNA fragment at the *Slr1* locus. The 6,026-bp inserted DNA fragment contains four truncated T-DNAs, including two copies of the *Hpt* genes with truncated 35S promoters (filled black boxes), the 595IPI fragment (blue bold line), and the *Xa27B* gene (purple arrow box), derived from the T-DNA region in the binary construct pC1300PP12. The two *Hpt* genes, with one on each side of the 6,026-bp inserted DNA fragment, were inserted in the opposite orientations. The 595IPI fragment was derived from the first intron of rice gene LOC_Os06g39760 (blue). LOC_Os06g39760 and the *Xa27B* gene are two adjacent genes with the same orientation in PP12, a genomic subclone located at 5,125-bp downstream of the *Xa27* gene cloned in the T-DNA region of pC1300PP12. However, the 595IPI fragment and the *Xa27B* gene were inserted in the opposite orientations and flanked by the two *Hpt* genes at the *Slr1* locus. The corresponding regions between the four truncated T-DNAs at the *Slr1* locus and the DNA elements in the T-DNA regions of pC1300PP12 are marked with dotted lines. For illustration purposes, only two copies of the T-DNA regions of pC1300PP12 were drawn. However, the four truncated T-DNAs at the *Slr1* locus might be derived from illegitimate integration of two to four copies of T-DNA in rice genome. Schematic maps in A and B are not drawn to scale. *Hpt*, hygromycin phosphotransferase gene; PP12, the 11,909-bp *Pst*I subclone located 5,125-bp downstream of the *Xa27* gene in IRBB27; P_{2x35S}, 2x35S promoter; $P_{t2x35S1}$, 398-bp truncated 2x35S promoter; $P_{t2x35S2}$, 583-bp truncated 2x35S promoter; P_{Xa27B}, *Xa27B* promoter; T_{Xa27B}, *Xa27B* terminator; T_{35S}, 35S terminator; 595IPI, the 595-bp DNA fragment derived from the first intron of rice gene LOC_Os06g39760; LB, left border; RB, right border.

dicated that the $P_{t2x35S1}$ promoter, inserted in reverse orientation and separated by the 595IPI fragment, activated the *Xa27B* gene in *Slr1* plants. Previous studies revealed that the 35S promoter harbors an enhancer element, and this 35S enhancer can potentiate promoter activity in reverse orientation (Kay et al. 1987; Noad et al. 1997). The P_{2x35S} promoter in pC1300 or pC1305.1 contains two tandem 35S enhancers sized 122 bp and 153 bp, respectively (Supplementary Fig. S4). The 153-bp 35S enhancer was still retained in the 398-bp truncated $P_{t2x35S1}$ promoter (Supplementary Fig. S4). To examine whether the P_{2x35S} promoter has promoter activity in reverse orientation, we deleted the P_{35S} promoter in front of the *GUS* gene in pC1305.1 to generate binary construct pC1305.1D1, in which the P_{2x35S} promoter was located upstream of the *GUS* gene in reverse orientation (Fig. 4). Indeed, GUS activity was detected in *N. benthamiana* leaves infiltrated with *Agrobacterium tumefaciens* strain GV3101 harboring pC1305.1D1 (Fig. 4). In addition, the P_{Xa27B}*:GUS:*T_{Nos} gene in pCXXP3 could still be activated in infiltrated *N. benthamiana* leaves by dTALE-Xa27B, a dTALE targeted to the putative TATA box in the *Xa27B* promoter (Fig. 4; Supplementary Fig. S3). The result indicates that the 412-bp P_{Xa27B} promoter is still functional as a core promoter, which can be activated by dTALE-Xa27B.

Characterization of *Xa27* paralog genes in IRBB27 and IR24

Four putative XA27 paralog proteins (BAD67963, BAD32947, BAD32948, and BAD32953) were identified from Nipponbare in the previous study, (Gu et al. 2005). They were annotated as LOC_Os06g07150, LOC_Os06g39800, LOC_Os06g39810, and LOC_Os06g39860 on chromosome 6, also designated as XAL2, XAL3, XAL1, and XAL4, respectively, in a previous study (Li et al. 2013; Supplementary Fig. S2). The IRBB27 alleles of the *Xa27* paralog genes were isolated and designated as *Xa27A*, *Xa27B*, *Xa27C* (*Xa27*), and *Xa27D*, respectively (Gu et al. 2005; Supplementary Figs. S2 and S5). Of the four *Xa27* paralog genes in IRBB27, *Xa27A* was mapped to the short arm of chromosome 6, while *Xa27B*, *Xa27*, and *Xa27D* are closely linked to each other and located at the *Xa27* locus on the long arm of chromosome 6 (Supplementary Fig. S2). The physical distance between *Xa27B* and *Xa27* is 6,107 bp, while *Xa27D* is located at 38,804 bp upstream of *Xa27*.

AvrXa27 binds to EBE_{AvrXa27} in the *Xa27* promoter and activates *Xa27* expression for disease resistance during incompatible interaction (Gu et al. 2005; Tian et al. 2014). In addition to the natural TAL effector gene *avrXa27*, we constructed three dTALE genes, *dTALE-Xa27A*, *dTALE-Xa27B*, and *dTALE-Xa27D*, whose products (dTALE-Xa27A, dTALE-Xa27B, and dTALE-Xa27D) specifically bind to $EBE_{\text{dTALE-Xa27A}}$, $EBE_{\text{dTALE-Xa27B}}$, and $EBE_{\text{dTALE-Xa27D}}$ in the promoters of *Xa27A*, *Xa27B*, and *Xa27D*, respectively (Fig. 5A). Cosmid constructs carrying *avrXa27* or dTALE genes were introduced into the *Xa27*-compatible *Xoo* strain 1947 and used for bacterial blight inoculation on IRBB27. IRBB27 conferred race-specific disease resistance to *Xoo* strains 1947(pHM1dTALE-Xa27B) and 1947(pHM1AvrXa27), respectively, but was susceptible to the *Xoo* strains harboring pHM1dTALE-Xa27A, pHM1dTALE-Xa27D, or the empty vector pHM1 (Fig. 5B). qRT-PCR analysis confirmed that *Xa27*, *Xa27B*, *Xa27A*, and *Xa27D* were specifically and efficiently induced by the *Xoo* strains harboring cosmid constructs carrying *avrXa27* or the corresponding dTALE genes (Fig. 5C). The results demonstrated that although *Xa27* and its paralog genes were efficiently induced by the cognate AvrXa27 or dTALE genes, only *Xa27* and *Xa27B* were functional, and their expression conferred disease resistance to the corresponding incompatible *Xoo* strains.

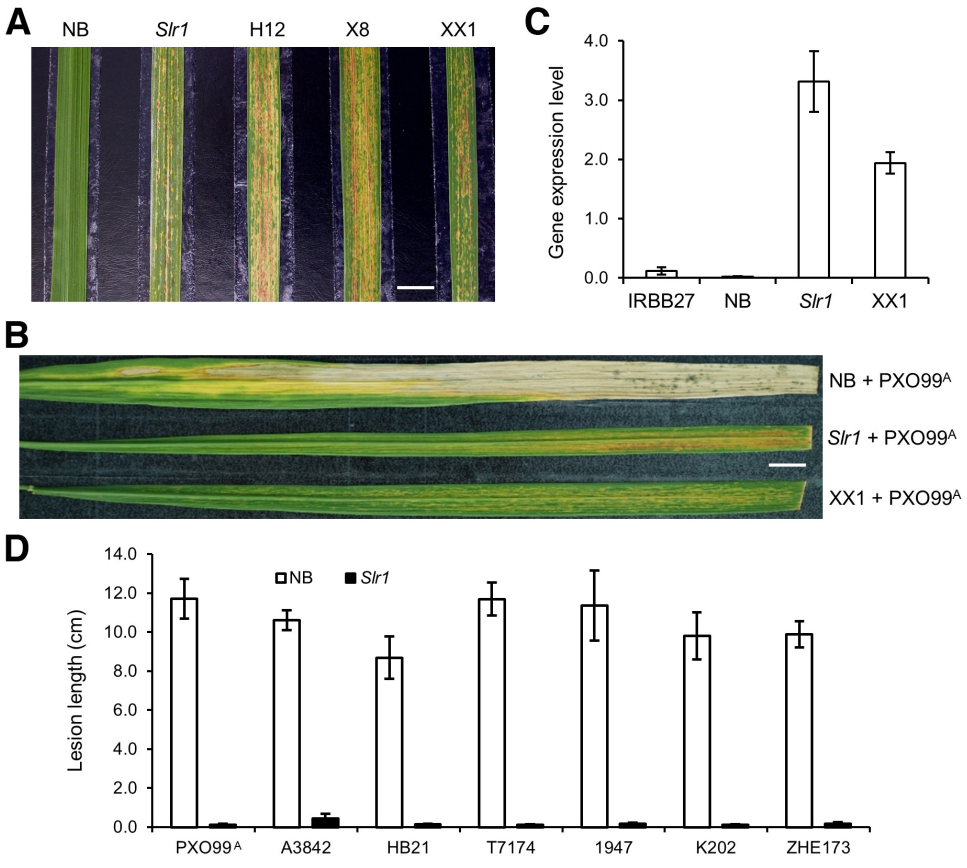

Fig. 3. Constitutive activation of *Xa27B* at the *Slr1* locus caused lesion mimic phenotype and conferred enhanced and broad-spectrum disease resistance to *Xanthomonas oryzae* pv. *oryzae* (*Xoo*). **A,** Lesion mimic phenotype of transgenic plants. H12, X8, and XX1, representative transgenic plants harboring subclones H20015, X8291, and XX2654, respectively. Scale bar: 1 cm. **B,** Bacterial blight phenotype of transgenic plants. Images of inoculated leaves were taken at 14 days after inoculation (DAI) with *Xoo* strain PXO99^{A}. Scale bar: 1 cm. **C,** Detection of *Xa27B* in IRBB27, Nipponbare (NB), *Slr1*, and XX1 plants by qRT-PCR. The gene expression level was normalized to rice elongation factor gene *OsEF-1α*. **D,** Lesion length of bacterial blight on Nipponbare and *Slr1* plants. Lesion lengths were measured at 14 DAI with *Xoo* strains.

IRBB27 is a near-isogenic line of the *Xa27* gene in the IR24 genetic background (Gu et al. 2004). Our previous study revealed that the *Xa27* alleles in IRBB27 and IR24 have an identical ORF but show polymorphism in their promoter regions (Gu et al. 2005). The IR24 alleles of the *Xa27A*, *Xa27B*, and *Xa27D* genes were isolated by PCR amplification and DNA sequencing. Both *Xa27A* and *Xa27B* have identical alleles in IR24 and IRBB27, respectively. Compared with the *Xa27D* allele in IRBB27, the *Xa27D* allele in IR24 has a three-nucleotide deletion in the coding region, encoding a hypothetical protein of 125 amino acid residues (Supplementary Fig. S6). Except for the IR24 allele of the *Xa27* gene, whose promoter does not have EBE for AvrXa27, the IR24 alleles of the *Xa27A*, *Xa27B*, and *Xa27D* genes have the corresponding EBEs in their promoters for dTALE-Xa27A, dTALE-Xa27B, and dTALE-Xa27D. IR24 was evaluated for disease resistance to *Xoo* strains harboring the *avrXa27* gene, the three dTALE genes, or pHM1. Bacterial blight inoculation showed that IR24 was resistant to 1947(pHM1dTALE-Xa27B), but susceptible to 1947(pHM1dTALE-Xa27A) and 1947(pHM1dTALE-Xa27D) (Supplementary Fig. S7). The results indicate that, of the three newly identified *Xa27* paralog genes in IRBB27 or IR24, only *Xa27B* encodes a functional R protein. In previous study, the *XAL3* gene, the *Xa27B* allele in Nipponbare, was activated by dTALE-XAL3; however, the induced *XAL3* gene could not confer resistance to the dTALE-XAL3-containing *Xoo* strain (Li et al. 2013). XA27B (115 aa) and XAL3 (114 aa) show 93.9% identity at the amino acid level (Supplementary Fig. S8). Compared with XA27B, there are one deletion and six substitutions in XAL3 (Supplementary Fig. S8). However, the significance of the deletion and substitutions in protein function in disease resistance remains to be determined.

To further confirm *Xa27B* function in disease resistance, we generated two *Xa27B* knockout mutants through CRISPR/Cas9-mediated gene editing. The two *Xa27B* knockout mutants had 40-bp (-40bp) and 2-bp (-GG) deletions in the ORF region, respectively, resulting in the frameshift mutation (Fig. 5D). The knockout mutation in the -40bp or -GG mutant did not cause any significant change in plant growth and development. Bacterial blight inoculation showed that, compared with IRBB27, both -40bp and -GG mutants abolished disease resistance to *Xa27B*-incompatible *Xoo* strain 1947(pHM1dTALE-Xa27B) (Fig. 5E). The results genetically confirm that *Xa27B* is a functional executor-type *R* gene in IRBB27 and IR24 that could confer disease resistance to bacterial blight when activated.

XA27B localizes to the nuclear envelope, endoplasmic reticulum, and apoplast

XA27 and its paralogs were predicted to contain an N-terminal domain rich in positively charged amino acid residues and two to three transmembrane helices (Gu et al. 2005; Supplementary Fig. S9). The N-terminal domain and the first transmembrane helix form a signal anchor-like sequence. Our previous

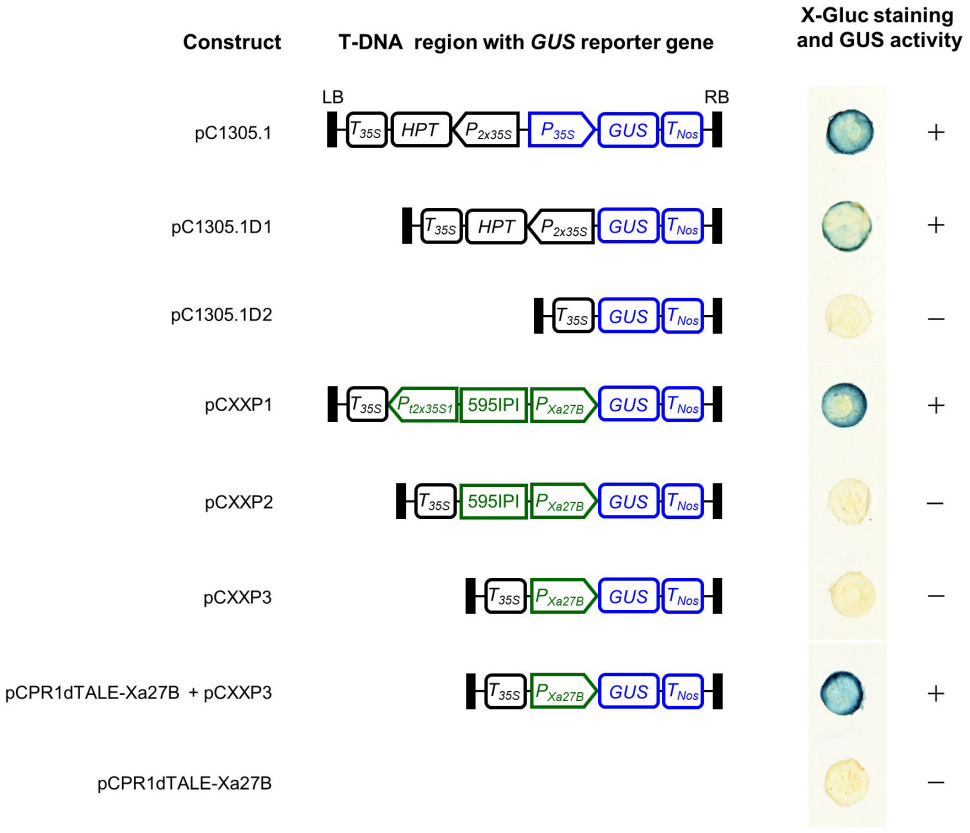

Fig. 4. Detection of promoter activity of the DNA elements upstream of the *Xa27B* gene at the *Slr1* locus. The promoter activity was indicated with expression of β-glucuronidase (GUS) activity in *Nicotiana benthamiana* leaf discs at 48 h after agroinfiltration with *Agrobacterium tumefaciens* GV3101 harboring binary constructs. The DNA elements in the T-DNA regions of binary constructs that contain GUS reporter genes are shown in the middle panel. The DNA elements shown in green were derived from the DNA sequence upstream of the *Xa27B* coding region in the subclone XX2654. Maps are not drawn to scale. GUS activity was detected by staining the infiltrated leaf discs with 5-bromo-4-chloro-3-indolyl-β-D-glucuronic acid (X-Gluc) solution. The infiltrated leaf discs stained in blue color were marked with a plus (+); otherwise, they are indicated with a minus (–) . LB, left border; RB, right border; T_{35S}, 35S terminator; *HPT*, hygromycin phosphotransferase gene; P_{2x35S}, 2x35S promoter; $P_{t2x35S1}$, the 398-bp truncated 2x35S promoter derived from the *Slr1* locus; P_{35S}, 35S promoter; *GUS*, *GUSPlus-His6* coding region; T_{Nos}, nopaline synthase terminator; 595IPI, the 595-bp DNA fragment at the *Slr1* locus derived from the first intron of rice gene LOC_Os06g39760; P_{Xa27B}, *Xa27B* promoter; pCPR1dTALE-Xa27B, binary construct harboring *dTALE-Xa27B* gene.

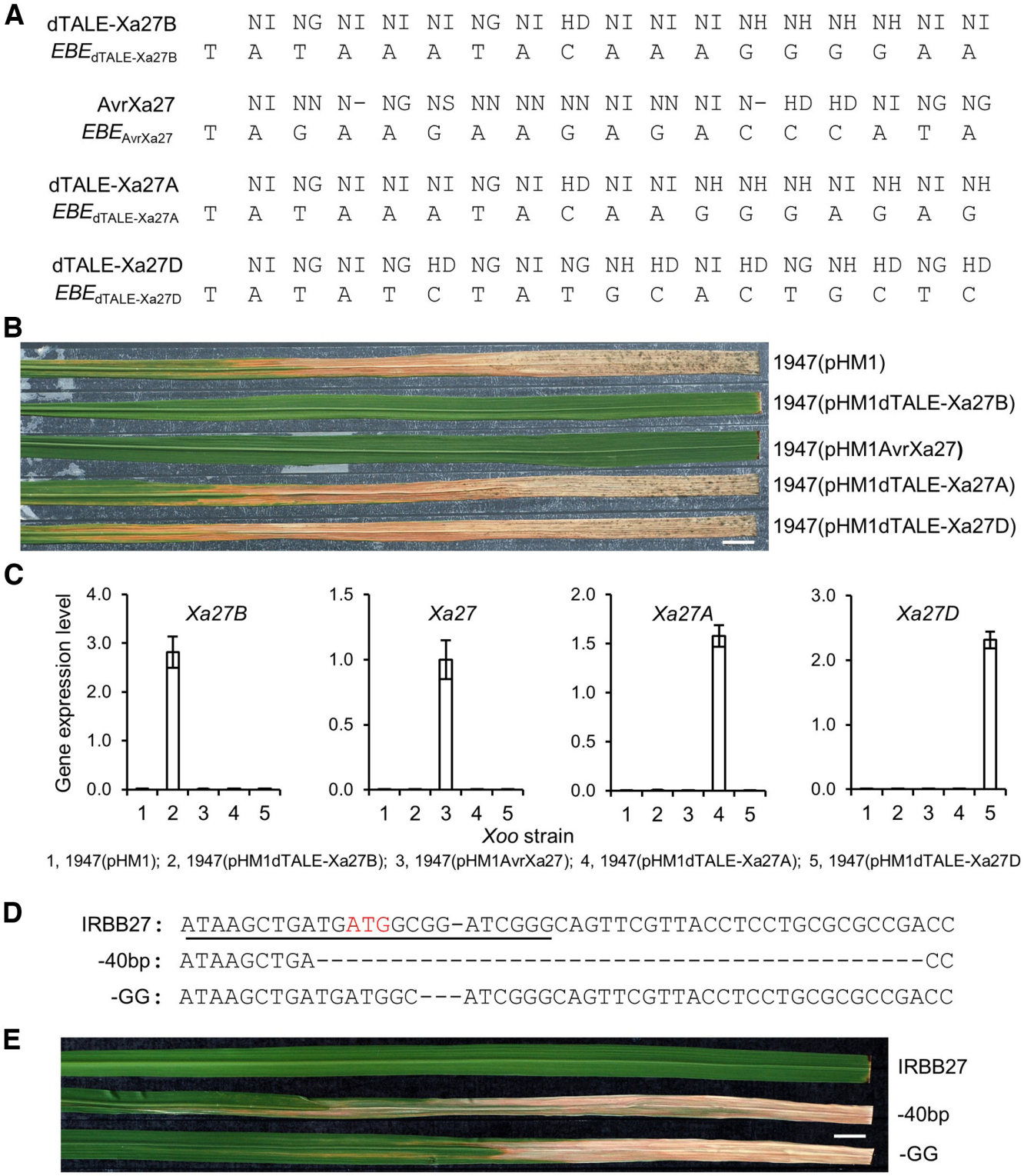

Fig. 5. Characterization of *Xa27* paralog genes in IRBB27. **A,** Repeat variable di-residues (RVDs) of designed transcription activator-like (TAL) effectors and DNA sequences of effector binding elements (*EBE*s). *EBE*s start with T at the "0" position. **B,** Bacterial blight phenotype of IRBB27 at 14 days after inoculation (DAI) with *Xanthomonas oryzae* pv. *oryzae* (*Xoo*) strains. Scale bar: 1 cm. **C,** Detection of expression of *Xa27B*, *Xa27*, *Xa27A*, and *Xa27D* in IRBB27 at 24 h after inoculation with *Xoo* strains harboring empty vector pHM1 or dTALE genes by qRT-PCR. The gene expression level was normalized to rice elongation factor gene *OsEF-1α*. **D,** Alignment of DNA sequences between IRBB27 and *Xa27B* knockout mutants. The target DNA of gRNA and protospacer adjacent motif (PAM) sequences in IRBB27 are underlined. The start codon "ATG" is shown in red. A hyphen (-) was introduced to achieve maximal alignment. **E,** Bacterial blight phenotype of IRBB27 and *Xa27B* knockout mutants at 2 weeks after inoculation with *Xoo* strain 1947 expressing dTALE-Xa27B. -40bp and -GG, *Xa27B* knockout mutants. Scale bar: 1 cm.

study demonstrated that XA27 depends on the N-terminal signal anchor-like sequence to localize to the apoplast of rice cells, which is required for disease resistance to *Xoo* (Wu et al. 2008). To investigate the subcellular localization of the XA27B protein in rice cells, we constructed an *Xa27B-GFP* fusion gene under the control of the 35S promoter (P_{35S}*:Xa27B-GFP:*T_{Nos}) and generated transgenic rice plants. Transgenic rice plants harboring the P_{35S}*:Xa27B-GFP:*T_{Nos} gene developed a lesion mimic phenotype similar to that of *Slr1* plants (Fig. 6A). The expression of the XA27B-GFP protein with the expected molecular size of 40.5 kilodaltons (kDa) was detected in the P_{35S}*:Xa27B-GFP:*T_{Nos} plants (Fig. 6B). The results suggested that, like XA27B, the XA27B-green fluorescent protein (GFP) fusion protein was functional and induced cell death when constitutively expressed in rice. We then examined the subcellular localization of XA27B-GFP in root cells of transgenic plants with or without plasmolysis induction. In untreated root cells, the XA27B-GFP signal was mainly observed in the nuclear envelope and marginal area (endoplasmic reticulum, plasma membrane, cell wall, or apoplast) of root cells (Fig. 6C). After plasmolysis induction in a high osmotic solution, the XA27-GFP signal on the cell walls or apoplast was still observed (Fig. 6C). By contrast, the control GFP signal was mainly localized to the cytosol and nucleus, and no GFP signal was observed on the cell walls and apoplast of root cells after plasmolysis induction (Fig. 6C). The results demonstrated that, like XA27, XA27B is localized to the cell wall and the apoplast and may be secreted to apoplast via exocytosis (Wu et al. 2008).

Discussion

So far, four executor-type *R* genes for bacterial blight resistance, namely *Xa7*, *Xa10*, *Xa23*, and *Xa27*, have been isolated from rice through positional cloning (Chen et al. 2021; Gu et al. 2005; Luo et al. 2021; Tian et al. 2014; Wang et al. 2015, 2021). In addition, two *Xa10*-like genes in Nipponbare, *Xa10-Ni* and *Xa23-Ni*, are also functional in conferring disease resistance to *Xoo* when they are activated (Wang et al. 2017). These executor-type *R* genes encode compact novel proteins with two to four transmembrane domains with unknown biochemical and biophysical functions. These rice executor-type R proteins exhibit no or low sequence identity to each other, except for XA10 and

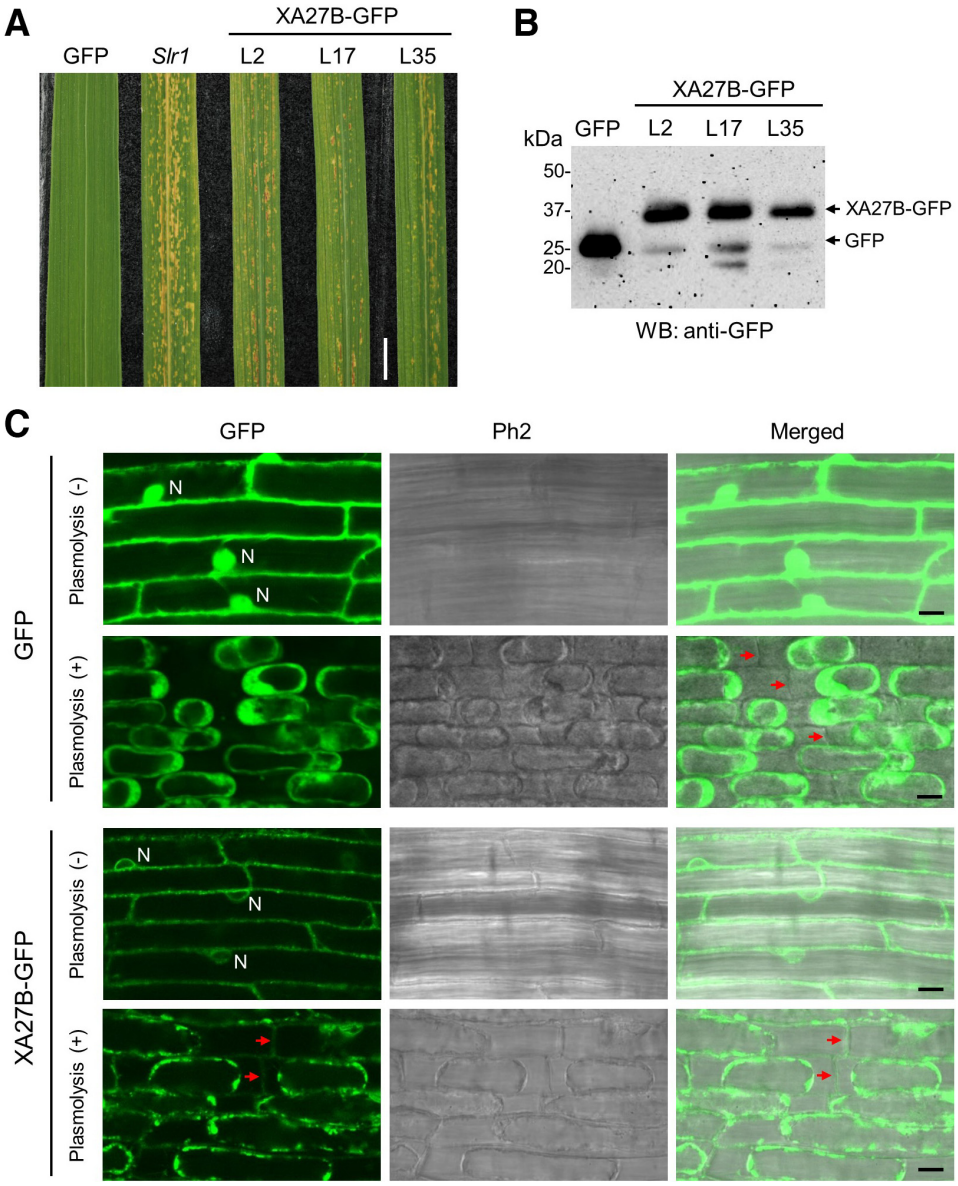

Fig. 6. Detection of XA27B-GFP (green fluorescent protein) subcellular localization in rice cells. **A,** Phenotype of Xa27B-GFP tagging lines. GFP, homozygous transgenic rice line harboring the P_{35S}*:GFP:*T_{Nos} gene; *Slr1*, *Xa27B* ectopic expression line; L2, L17, and L35, independent homozygous transgenic rice lines harboring the P_{35S}*:Xa27B-GFP:*T_{Nos} gene. Scale bar: 1 cm. **B,** Expression of XA27B-GFP proteins in transgenic plants. GFP and XA27B-GFP were detected by Western blot analysis using anti-GFP antibody. **C,** Subcellular localization of XA27B-GFP in rice cells. Images were taken under a confocal microscope with root cells of transgenic plants harboring the P_{35S}*:GFP:*T_{Nos} gene (top panels) or the P_{35S}*:Xa27B-GFP:*T_{Nos} gene (bottom panels). Cell walls of root cells after plasmolysis induction are indicated with red arrowheads. N, Nuclei; Ph2, Phase Contrast 2. Scale bars: 10 μm.

XA23, which are paralogs (Wang et al. 2017; Zhang et al. 2015). The isolation of these executor-type *R* genes relied heavily on subcloning and genetic complementation, as they could not be predicted at the fine mapping stages (Gu et al. 2004, 2008; Wang et al. 2014). Although the *Xa27B* gene is located at only 6,107 bp downstream of the *Xa27* gene in IRBB27, the genomic subclone PP12 only harbors the *Xa27B* gene. Among 60 T0 plants derived from the transformation study with the PP12 subclone, most of them should carry the *Xa27B* gene. However, because of the absence of cognate TAL effector gene in *Xoo* strain PXO99^{A} for the *Xa27B* gene, the resistance specificity of *Xa27B* could not be identified or characterized in *Xa27* complementation study. The *Slr1* line was initially characterized as a lesion mimic mutant. The genetic complementation with subclones at the *Slr1* locus and gene expression analysis narrowed the candidate gene down to the *Xa27B* gene responsible for the lesion mimic phenotype (Figs. 2A and 3A). The function of the *Xa27B* gene was further confirmed by the induction of the *Xa27B* in IRBB27 by dTALE-Xa27B and disease evaluation for bacterial blight resistance (Fig. 5A to C). IR24 was found to harbor an identical allele of the *Xa27B* gene to that in IRBB27, which is functional for disease resistance to *Xoo* when activated (Supplementary Fig. S7). In the future, IR24 may be used to screen for incompatible *Xoo* strains that may harbor the cognate TAL effector genes for the *Xa27B* gene.

Like the expression of other executor-type *R* genes in rice, the expression of the *Xa27B* gene in IRBB27 is tightly regulated (Fig. 3C). Although the 412-bp P_{Xa27B} promoter did not show full promoter activity in the transient assay of GUS activity in *N. benthamiana*, the *Xa27B* gene at the *Slr1* locus with the P_{Xa27B} promoter was constitutively expressed (Figs. 3C and 4). Ectopic expression of *Xa27* transgenes was also observed in the complementation study of the *Xa27* gene under the control of its native promoter (Gu et al. 2005). A few transgenic plants harboring *Xa27* genomic clone NN9.9 or NA3.2 showed constitutive expression of the *Xa27* gene and conferred enhanced and broad-spectrum disease resistance to both *Xa27*-incompatible and *Xa27*-compatible *Xoo* strains (Gu et al. 2005). Considering that not all the transgenic plants showed ectopic expression of *Xa27* or *Xa27B* transgenes, we initially speculated that the ectopic expression of the transgenes in these lines might be caused by the position effect or other unknown reasons at the T-DNA insertion sites. Using a promoter-less GUS reporter system, we learned that it should be the 398-bp truncated $P_{t2x35S1}$ promoter harboring a 35S enhancer in reverse orientation rather than the 412-bp *Xa27B* promoter alone that activated the *Xa27B* gene at the *Slr1* locus (Fig. 4). The ectopic expression of the *Xa27B* gene at the *Slr1* locus resulted from the illegitimate integration of multiple truncated T-DNAs, which should be considered an isolated case. Nevertheless, the characterization of the *Xa27B* ectopic expression line *Slr1* provided us an opportunity to identify the functional *Xa27* paralog gene *Xa27B* in IRBB27 and IR24, especially when the *XAL3* gene, the corresponding *Xa27B* allele in Nipponbare, was tested to be nonfunctional in disease resistance to *Xoo* when activated by dTALE-XAL3 (Li et al. 2013).

The functional XA27B-GFP was found to localize to the nuclear envelope, endoplasmic reticulum, cell wall, and apoplast (Fig. 6C), which was similar to XA27-GFP localization (Wu et al. 2008). Previously, XA27-FLAG was detected in both cytoplasmic electron-dense vesicles and apoplast by immunogold electron microscopy examination (Wu et al. 2008). It is speculated that XA27B, like XA27, might be synthesized on the endoplasmic reticulum and secreted to the apoplast through Golgi-derived vesicles (Wu et al. 2008). The apoplast is a compartment that includes the cell wall and the space between the cell wall and the plasma membrane. It plays an important role in plant development and in response to various biotic and abiotic stresses. During pathogen–host cell interaction, most plant pathogenic microorganisms actively penetrate the plant apoplast to access intracellular nutrients. However, on the host side, plants can protect themselves from pathogenic invasion in at least three ways: inhibiting cell wall degradation (Aparna et al. 2009; Kachewar et al. 2019; Sinha et al. 2013), structurally and chemically remodeling the cell wall (Gu et al. 2005; Hilaire et al. 2001; Tian and Yin 2009), and killing pathogens by producing antibacterial agents or toxic chemicals (Tiku 2018; Wojtaszek 1997). Although the detailed biochemical function of Xa27B on the cell wall and apoplast remains to be investigated, constitutive expression of *Xa27B* in *Slr1* plants resulted in ROS generation, which would contribute to cell wall thickening through lignification. Our previous studies showed that the induced XA27 in IRBB27 plants during incompatible interaction or in *Xa27* ectopic expression lines caused secondary cell wall thickening and reduced pit diameter in rice (Gu et al. 2005; Tian and Yin 2009). As one of the most important HR components, ROS generation not only causes cell death, but also suppresses or kills pathogens directly (Hilaire et al. 2001; Wojtaszek 1997). All these defense reactions enable *Slr1* plants to confer enhanced and broad-spectrum resistance to *Xoo* and *Xoc* strains (Figs. 1B to G and 3D).

Both *indica* and *japonica* subspecies of rice harbor the four *Xa27* paralog genes, suggesting that they might have already been present in rice before the subspecification of *indica* and *japonica* rice. However, only the alleles of the *Xa27* and *Xa27B* genes in IRBB27 and IR24 could confer disease resistance to *Xoo* when activated (Gu et al. 2005; Li et al. 2013; Fig. 5A to C). Other *Xa27* paralog genes in *indica* or *japonica*, including the *XAL3* allele in Nipponbare, do not evolve this function or abolish this function during evolution. Although the exact evolutionary origin of the executor-type *R* genes in rice is still unclear, it is tempting to speculate that these executor-type *R* genes in rice might evolve from ancient genes that were involved in developmental programmed cell death (Nowack et al. 2022). Two *Xa27B* knockout mutants were generated in this study. But they did not show any significant change in growth and development, except for the loss of disease resistance to incompatible *Xoo* strains (Fig. 5E). However, as there are four *Xa27* paralog genes present in the rice genome and their function may have redundancy, more detailed genetic studies, especially gene editing work, need to be done to investigate whether these *Xa27* paralog genes have a function in plant growth and development or stress response. Nevertheless, the identification of the *Xa27B* gene as a new functional executor-type *R* gene provides additional genetic resources for studying the mechanism of executor-type R protein-mediated ETI and generating enhanced and broad-spectrum disease resistance to *Xoo* through promoter engineering (Zeng et al. 2015).

Materials and Methods

Constructs and strains

The central repeats in dTALE-Xa27A, dTALE-Xa27B, and dTALE-Xa27D were designed according to the codes between RVDs and DNA nucleotides (NI = A, NG = T, HD = C, NN/NH = G) (Boch et al. 2009). The repeats of dTALEs were assembled and cloned into vector pTAL1 according to a method described previously (Cermak et al. 2011). The *Sph*I fragments of central DNA repeats in dTALEs were isolated and used to replace the central DNA repeats of *avrXa27* in pZWavrXa27 to generate pZWdTALE-Xa27A, pZWdTALE-Xa27B, and pZWdTALE-Xa27D, respectively. The constructs were then digested with *Hind*III and inserted into the *Hind*III site of cosmid vector pHM1 (GenBank accession no. EF059993) to generate constructs pHM1dTALE-Xa27A, pHM1dTALE-

Xa27B, and pHM1dTALE-Xa27D. The cosmid constructs were transferred into *Xoo* strain 1947 by electroporation.

A homemade BAC library of *Slr1* was generated in pIndigoBAC-5 as previously described (Wang et al. 1995). A BAC clone M180P19 was identified from the BAC library using a DNA probe derived from the rice genome sequence flanking the *Slr1* locus and sequenced. Subclones derived from the M180P09 were cloned into binary vector pCAMBIA-1300 (pC1300) (GenBank accession no. AF234296). A specific DNA target sequence and its adjacent protospacer adjacent motif (PAM) (ATAAGCT GATGATGGCGGATCGGG) were designed for CRISPR/Cas9-mediated gene editing of the coding region in *Xa27B*. An expression cassette containing the target sequence and the gRNA under rice snRNA U3 promoter in vector pYLgRNA was amplified and cloned into vector pYLCRISPR/Cas9PUbi-H to generate binary construct pYLCas9-Xa27B, according to a previously described method (Ma et al. 2015). The oligo primers for construct making were Xa27BU3-F and Xa27BU3-R (Supplementary Table S1). The oligo primers for PCR amplification and DNA sequencing of the target site and its flanking regions in *Xa27B* were Xa27B-Seq-F2 and Xa27B-Seq-R2 (Supplementary Table S1). The coding region of the *Xa27B* gene was amplified using primers Xa27PB-KpnI-F and Xa27PB-BamHI-R (Supplementary Table S1). The PCR product was double digested with *Kpn*I and *Bam*HI and inserted into pC35S-GFP to generate pC35S-Xa27B-GFP (Tian et al. 2014). The binary constructs were introduced into *A. tumefaciens* stain AGL1 and used for rice transformation.

Binary vector pCAMBIA-1305.1 (pC1305.1) (GenBank accession no. AF354045) was used as the positive control for the detection of GUS activity. The CaMV35S promoter (35S promoter or P_{35S}) for the *GUS* gene in pC1305.1 was deleted to generate pC1305.1D1. The CaMV35Sx2 promoter (2x35S promoter or P_{2x35S}) and the *Hpt* coding region in pC1305.1D1 were further deleted to produce pC1305.1D2. The $P_{t2x35S1}$-595IPI-P_{Xa27B}, 595IPI-P_{Xa27B}, and P_{Xa27B} fragments derived from the inserted region upstream of the *Xa27B* coding region at the *Slr1* locus were inserted into the upstream of the *GUS* gene in pC1305.1D2 to generate pCXXP1, pCXXP2, and pCXXP3, respectively. The central repeat region of the *avrXa27* gene in pCPR1avrXa27 (Tian and Yin 2009) was replaced with the 3,240-bp *Bam*HI fragment from pZWdTALE-Xa27B to generate pCPR1dTALE-Xa27B for the transient expression of the *dTALE-Xa27B* gene in *N. benthamiana*. The binary constructs were introduced into *A. tumefaciens* stain GV3101 and used for agroinfiltration on *N. benthamiana*.

Rice transformation and rice growth condition

Rice cultivar Nipponbare, a cultivar susceptible to the *Xa27*-incompatible *Xoo* strain PXO99^{A}, was chosen for the complementation study. *Agrobacterium*-mediated transformation of Nipponbare was performed according to a previously described method (Hiei et al. 1994). Rice plants were grown in pot soil in a greenhouse with daylight at 12 to 12.5 h, temperature at 25 to 35°C, and relative humidity at 80 to 85%.

Bacterial blight inoculation

The *Xoo* and *Xoc* strains were cultured on a peptone sucrose agar (PSA) medium with appropriate antibiotics (10 g liter^{-1} peptone, 10 g liter^{-1} Suc, 1 g liter^{-1} Glu, and 16 g liter^{-1} bacto-agar, pH 7.0) for 2 to 3 d at 28°C. Bacteria were collected and suspended in sterile water at an optical density of 0.5 at 600 nm. Bacterial inoculations were conducted according to previously described methods (Tian and Yin 2009). The bacterial blight phenotypes were scored as resistant (R, Lesion length $\leq$ 3.0 cm), moderately resistant (MR, 3.0 cm $<$ Lesion length $<$ 6.0 cm), moderately susceptible (MS, 6.0 cm $<$ Lesion length $\leq$ 9.0 cm) and susceptible (S, Lesion length $>$ 9.0 cm).

Northern blot analysis, RACEs, and qRT-PCR

Northern blot analysis was carried out according to the procedures described previously (Tian and Yin 2009). Briefly, total RNA was isolated from rice leaves using the RNeasy Plant Mini Kit (Qiagen). Approximately 30 μg of total RNA was used for each lane in Northern blot analysis. The RNA loading was assessed by staining RNA blots with methylene blue. The probes for *PBZ1* and *PR1* genes were derived cDNA clones of the two genes. The full length of *Xa27B* cDNA was obtained by 5′ and 3′ RACE (Rapid Amplification of cDNA Ends) methods, as described previously (Tian et al. 2014). The PCR products were cloned into a pGEMT-easy vector (Promega) and sequenced. The specific primers for 5′ RACE and 3′ RACE were Xa27BRACE-F and Xa27BRACE-R, respectively (Supplementary Table S1). Total RNAs for qRT-PCR were isolated from leaves of 4-week-old rice plants at 24 h after infiltration with *Xoo* strains. qRT-PCR was carried out in accordance with previously described procedures (Tian et al. 2014). The expression of rice elongation factor (EF) gene *OsEF-1*α (Os03g0178000) was used as the internal control. The experiments were performed in triplicate and the data are presented as mean ± SD. The specific primers for all genes are listed as Supplementary Table S1.

Trypan blue and DAB staining

Trypan blue and DAB staining were carried out according to Tian et al. (2014). Briefly, leaves from 3-week-old rice plants were submerged in a 70°C trypan blue solution (2.5 mg of trypan blue ml^{-1}, 25% [wt/vol] lactic acid, 23% water-saturated phenol, and 25% glycerol) and boiled in water for 2 min and left at 37°C overnight for staining. The samples were photographed after destaining in chloral hydrate solution (25 g in 10 ml of water) for 3 to 7 days. Accumulation of H_2O_2 in rice leaves was detected using the DAB-uptake method with slight modification. Leaves from 3-week-old plants were placed in DAB solution (Sigma) and incubated at 25°C for 8 h. The samples were cleared by boiling in 96% ethanol for 10 min to 1 h. The cleared samples were mounted in 30% glycerol and 30% lactic acid for microscopic examination.

Confocal laser-scanning microscopy

GFP fluorescence in root cells of transgenic plants (GFP and XA27B-GFP L35) was examined with a confocal microscope (Zeiss LSM 510 META) using the excitation/emission combination of 488/505- to 530-nm bandpass. The bright-field image was taken simultaneously using Phase Contrast 2 optics. Plasmolysis was induced on root cells by incubating the samples in 10% (wt/vol) mannitol solution for 1 h and mounting them in the same solution for examination.

X-Gluc staining of GUS activity

Leaves of 3-week-old *N. benthamiana* were infiltrated as previously described (Tian et al. 2014). The β-glucuronidase (GUS) activity was assayed at 48 h post-agroinfiltration according to procedures previously described with slight modification (Hiei et al. 1994). The infiltrated leaves were incubated in phosphate buffer (50 mM NaPO4, pH 6.8) that contained 1% Triton X-100 at 37°C for 1 h. The solution was replaced with fresh phosphate buffer containing 1.0 mM 5-bromo-4-chloro-3-indolyl-β-D-glucuronic acid (X-Gluc) and 20% methanol. Samples were placed under a mild vacuum for 5 min, then incubated overnight at 37°C. Samples were washed with 70% ethanol several times before the visual examination.

Western blot analysis

Total proteins were isolated from leaves of 5-week-old rice plants as previously described (Nelson et al. 1984). About 20 μg of total protein was separated on a 10% sodium dodecylsulphate polyacrylamide gel, followed by blotting onto PVDF membranes. GFP and Xa27B-GFP were detected with anti-GFP antibody from Proteintech.

Acknowledgments

We thank Yao-Guang Liu for plant binary vector pYLCRISPR/Cas9Pubi-H, Ko Shimamoto for cDNA clones of the *PR1* and *PBZ1* gene, Xianming Zeng for *Xoc* strain L8, and Yuejing Gui and Raji Mohan for critical reading of the manuscript.

Literature Cited

Antony, G., Zhou, J., Huang, S., Li, T., Liu, B., White, F., and Yang, B. 2010. Rice *xa13* recessive resistance to bacterial blight is defeated by induction of the disease susceptibility gene Os-*11N3*. Plant Cell 22: 3864-3876.

Aparna, G., Chatterjee, A., Sonti, R. V., and Sankaranarayanan, R. 2009. A cell wall-degrading esterase of *Xanthomonas oryzae* requires a unique substrate recognition module for pathogenesis on rice. Plant Cell 21:1860-1873.

Balint-Kurti, P. 2019. The plant hypersensitive response: Concepts, control and consequences. Mol. Plant Pathol. 20:1163-1178.

Bigeard, J., Colcombet, J., and Hirt, H. 2015. Signaling mechanisms in pattern-triggered immunity (PTI). Mol. Plant 8:521-539.

Boch, J., Scholze, H., Schornack, S., Landgraf, A., Hahn, S., Kay, S., Lahaye, T., Nickstadt, A., and Bonas, U. 2009. Breaking the code of DNA binding specificity of TAL-type III effectors. Science 326:1509-1512.

Bogdanove, A. J., Schornack, S., and Lahaye, T. 2010. TAL effectors: Finding plant genes for disease and defense. Curr. Opin. Plant Biol. 13:394-401.

Cermak, T., Doyle, E. L., Christian, M., Wang, L., Zhang, Y., Schmidt, C., Baller, J. A., Somia, N. V., Bogdanove, A. J., and Voytas, D. F. 2011. Efficient design and assembly of custom TALEN and other TAL effector-based constructs for DNA targeting. Nucleic Acids Res. 39:e82.

Chen, X., Liu, P., Mei, L., He, X., Chen, L., Liu, H., Shen, S., Ji, Z., Zheng, X., Zhang, Y., Gao, Y., Zeng, D., Qian, Q., and Ma, B. 2021. *Xa7*, a new executor *R* gene that confers durable and broad-spectrum resistance to bacterial blight disease in rice. Plant Commun. 2:100143.

Chu, Z., Yuan, M., Yao, J., Ge, X., Yuan, B., Xu, C., Li, X., Fu, B., Li, Z., Bennetzen, J. L., Zhang, Q., and Wang, S. 2006. Promoter mutations of an essential gene for pollen development result in disease resistance in rice. Genes Dev. 20:1250-1255.

Gu, K., Sangha, J. S., Li, Y., and Yin, Z. 2008. High-resolution genetic mapping of bacterial blight resistance gene *Xa10*. Theor. Appl. Genet. 116:155-163.

Gu, K., Tian, D., Yang, F., Wu, L., Sreekala, C., Wang, D., Wang, G.-L., and Yin, Z. 2004. High-resolution genetic mapping of *Xa27(t)*, a new bacterial blight resistance gene in rice, *Oryza sativa* L. Theor. Appl. Genet. 108:800-807.

Gu, K., Yang, B., Tian, D., Wu, L., Wang, D., Sreekala, C., Yang, F., Chu, Z., Wang, G.-L., White, F. F., and Yin, Z. 2005. *R* gene expression induced by a type-III effector triggers disease resistance in rice. Nature 435:1122-1125.

Hiei, Y., Ohta, S., Komari, T., and Kumashiro, T. 1994. Efficient transformation of rice (*Oryza sativa* L.) mediated by *Agrobacterium* and sequence analysis of the boundaries of the T-DNA. Plant J. 6:271-282.

Hilaire, E., Young, S. A., Willard, L. H., McGee, J. D., Sweat, T., Chittoor, J. M., Guikema, J. A., and Leach, J. E. 2001. Vascular defense responses in rice: Peroxidase accumulation in xylem parenchyma cells and xylem wall thickening. Mol. Plant-Microbe Interact. 14: 1411-1419.

Kachewar, N. R., Gupta, V., Ranjan, A., Patel, H. K., and Sonti, R. V. 2019. Overexpression of OsPUB41, a rice E3 ubiquitin ligase induced by cell wall degrading enzymes, enhances immune responses in rice and Arabidopsis. BMC Plant Biol. 19:530.

Kay, R., Chan, A., Daly, M., and McPherson, J. 1987. Duplication of CaMV 35 S promoter sequences creates a strong enhancer for plant genes. Science 236:1299-1302.

Li, T., Huang, S., Zhou, J., and Yang, B. 2013. Designer TAL effectors induce disease susceptibility and resistance to *Xanthomonas oryzae* pv. *oryzae* in rice. Mol. Plant 6:781-789.

Lorrain, S., Vailleau, F., Balagué, C., and Roby, D. 2003. Lesion mimic mutants: Keys for deciphering cell death and defense pathways in plants? Trends Plant Sci. 8:263-271.

Luo, D., Huguet-Tapia, J. C., Raborn, R. T., White, F. F., Brendel, V. P., and Yang, B. 2021. The *Xa7* resistance gene guards the rice susceptibility gene *SWEET14* against exploitation by the bacterial blight pathogen. Plant Commun. 2:100164.

Ma, X., Zhang, Q., Zhu, Q., Liu, W., Chen, Y., Qiu, R., Wang, B., Yang, Z., Li, H., Lin, Y., Xie, Y., Shen, R., Chen, S., Wang, Z., Chen, Y., Guo, J., Chen, L., Zhao, X., Dong, Z., and Liu, Y.-G. 2015. A robust CRISPR/Cas9 system for convenient, high-efficiency multiplex genome editing in monocot and dicot plants. Mol. Plant 8:1274-1284.

Moscou, M. J., and Bogdanove, A. J. 2009. A simple cipher governs DNA recognition by TAL effectors. Science 326:1501.

Nelson, T., Harpster, M. H., Mayfield, S. P., and Taylor, W. C. 1984. Light-regulated gene expression during maize leaf development. J. Cell Biol. 98:558-564.

Ngou, B. P. M., Ahn, H.-K., Ding, P., and Jones, J. D. G. 2021. Mutual potentiation of plant immunity by cell-surface and intracellular receptors. Nature 592:110-115.

Ngou, B. P. M., Ding, P., and Jones, J. D. 2022. Thirty years of resistance: Zig-zag through the plant immune system. Plant Cell 34: 1447-1478.

Niño-Liu, D. O., Ronald, P. C., and Bogdanove, A. J. 2006. *Xanthomonas oryzae* pathovars: Model pathogens of a model crop. Mol. Plant Pathol. 7:303-324.

Noad, R. J., Turner, D. S., and Covey, S. N. 1997. Expression of functional elements inserted into the 35S promoter region of infectious cauliflower mosaic virus replicons. Nucleic Acids Res. 25:1123-1129.

Nowack, M. K., Holmes, D. R., and Lahaye, T. 2022. TALE-induced cell death executors: An origin outside immunity? Trends Plant Sci. 27:536-548.

Sinha, D., Gupta, M. K., Patel, H. K., Ranjan, A., and Sonti, R. V. 2013. Cell wall degrading enzyme induced rice innate immune responses are suppressed by the type 3 secretion system effectors XopN, XopQ, XopX and XopZ of *Xanthomonas oryzae* pv. *oryzae*. PLoS One 8:e75867.

Sugio, A., Yang, B., Zhu, T., and White, F. F. 2007. Two type III effector genes of *Xanthomonas oryzae* pv. *oryzae* control the induction of the host genes *OsTFIIAγ1* and *OsTFX1* during bacterial blight of rice. Proc. Natl. Acad. Sci. U.S.A. 104:10720-10725.

Tang, X., Xie, M., Kim, Y. J., Zhou, J., Klessig, D. F., and Martin, G. B. 1999. Overexpression of *Pto* activates defense responses and confers broad resistance. Plant Cell 11:15-29.

Tian, D., Wang, J., Zeng, X., Gu, K., Qiu, C., Yang, X., Zhou, Z., Goh, M., Luo, Y., Murata-Hori, M., White, F. F., and Yin, Z. 2014. The rice TAL effector-dependent resistance protein XA10 triggers cell death and calcium depletion in the endoplasmic reticulum. Plant Cell 26: 497-515.

Tian, D., and Yin, Z. 2009. Constitutive heterologous expression of *avrXa27* in rice containing the *R* gene *Xa27* confers enhanced resistance to compatible *Xanthomonas oryzae* strains. Mol. Plant Pathol. 10:29-39.

Tiku, A. R. 2018. Antimicrobial Compounds and Their Role in Plant Defense. Springer, Singapore.

Wang, C., Chen, S., Feng, A., Su, J., Wang, W., Feng, J., Chen, B., Zhang, M., Yang, J., Zeng, L., and Zhu, X. 2021. *Xa7*, a small orphan gene harboring promoter trap for AvrXa7, leads to the durable resistance to *Xanthomonas oryzae* pv. *oryzae*. Rice 14:48.

Wang, C., Fan, Y., Zheng, C., Qin, T., Zhang, X., and Zhao, K. 2014. High-resolution genetic mapping of rice bacterial blight resistance gene *Xa23*. Mol. Genet. Genomics 289:745-753.

Wang, C., Zhang, X., Fan, Y., Gao, Y., Zhu, Q., Zheng, C., Qin, T., Li, Y., Che, J., Zhang, M., Yang, B., Liu, Y., and Zhao, K. 2015. XA23 is an executor R protein and confers broad-spectrum disease resistance in rice. Mol. Plant 8:290-302.

Wang, G. L., Holsten, T. E., Song, W. Y., Wang, H. P., and Ronald, P. C. 1995. Construction of a rice bacterial artificial chromosome library and identification of clones linked to the *Xa-21* disease resistance locus. Plant J. 7:525-533.

Wang, J., Tian, D., Gu, K., Yang, X., Wang, L., Zeng, X., and Yin, Z. 2017. Induction of *Xa10*-like genes in rice cultivar Nipponbare confers disease resistance to rice bacterial blight. Mol. Plant-Microbe Interact. 30:466-477.

Wojtaszek, P. 1997. Oxidative burst: An early plant response to pathogen infection. Biochem. J. 322:681-692.

Wu, L., Goh, M. L., Sreekala, C., and Yin, Z. 2008. XA27 depends on an amino-terminal signal-anchor-like sequence to localize to the apoplast for resistance to *Xanthomonas oryzae* pv *oryzae*. Plant Physiol. 148:1497-1509.

Yang, B., Sugio, A., and White, F. F. 2006. *Os8N3* is a host disease-susceptibility gene for bacterial blight of rice. Proc. Natl. Acad. Sci. U.S.A. 103:10503-10508.

Yang, B., and White, F. F. 2004. Diverse members of the AvrBs3/PthA family of type III effectors are major virulence determinants in bacterial blight disease of rice. Mol. Plant-Microbe Interact. 17:1192-1200.

Yuan, M., Jiang, Z., Bi, G., Nomura, K., Liu, M., Wang, Y., Cai, B., Zhou, J.-M., He, S. Y., and Xin, X.-F. 2021. Pattern-recognition receptors are required for NLR-mediated plant immunity. Nature 592:105-109.

Zeng, X., Tian, D., Gu, K., Zhou, Z., Yang, X., Luo, Y., White, F. F., and Yin, Z. 2015. Genetic engineering of the *Xa10* promoter for broad-spectrum and durable resistance to *Xanthomonas oryzae* pv. *oryzae*. Plant Biotechnol. J. 13:993-1001.

Zhang, A., Jiang, H., Chu, H., Cao, L., and Chen, J. 2022. Rice lesion mimic gene cloning and association analysis for disease resistance. Curr. Issues Mol. Biol. 44:2350-2361.

Zhang, J., Yin, Z., and White, F. 2015. TAL effectors and the executor *R* genes. Front. Plant Sci. 6:641.